

Maryam Bamshad, Victor T. Aoki, M. Gregory Adkison, Wade S. Warren and Timothy J. Bartness

Am J Physiol Regulatory Integrative Comp Physiol 275:291-299, 1998.

You might find this additional information useful...

This article cites 37 articles, 8 of which you can access free at:

<http://ajpregu.physiology.org/cgi/content/full/275/1/R291#BIBL>

This article has been cited by 28 other HighWire hosted articles, the first 5 are:

Anterograde transneuronal viral tract tracing reveals central sensory circuits from white adipose tissue

C. K. Song, G. J. Schwartz and T. J. Bartness

Am J Physiol Regulatory Integrative Comp Physiol, March 1, 2009; 296 (3): R501-R511.

[Abstract] [Full Text] [PDF]

Antagonism of specific corticotropin-releasing factor receptor subtypes selectively modifies weight loss in restrained rats

C. Chotiawat and R. B. S. Harris

Am J Physiol Regulatory Integrative Comp Physiol, December 1, 2008; 295 (6): R1762-R1773.

[Abstract] [Full Text] [PDF]

Melanocortin-4 receptor mRNA expressed in sympathetic outflow neurons to brown adipose tissue: neuroanatomical and functional evidence

C. K. Song, C. H. Vaughan, E. Keen-Rhinehart, R. B. S. Harris, D. Richard and T. J. Bartness

Am J Physiol Regulatory Integrative Comp Physiol, August 1, 2008; 295 (2): R417-R428.

[Abstract] [Full Text] [PDF]

Differential sympathetic drive to adipose tissues after food deprivation, cold exposure or glucoprivation

N. A. Brito, M. N. Brito and T. J. Bartness

Am J Physiol Regulatory Integrative Comp Physiol, May 1, 2008; 294 (5): R1445-R1452.

[Abstract] [Full Text] [PDF]

Food deprivation-induced changes in body fat mobilization after neonatal monosodium glutamate treatment

C. Leitner and T. J. Bartness

Am J Physiol Regulatory Integrative Comp Physiol, March 1, 2008; 294 (3): R775-R783.

[Abstract] [Full Text] [PDF]

Medline items on this article's topics can be found at <http://highwire.stanford.edu/lists/artbytopic.dtl> on the following topics:

Medicine .. Lipid Mobilization
Neuroscience .. Central Nervous System
Veterinary Science .. Spinal Cord
Veterinary Science .. Sympathetic Nervous System
Medicine .. Adipose Tissue
Physiology .. Rats

Updated information and services including high-resolution figures, can be found at:

<http://ajpregu.physiology.org/cgi/content/full/275/1/R291>

Additional material and information about *American Journal of Physiology - Regulatory, Integrative and Comparative Physiology* can be found at:

<http://www.the-aps.org/publications/ajpregu>

This information is current as of November 28, 2009 .

The American Journal of Physiology - Regulatory, Integrative and Comparative Physiology publishes original investigations that illuminate normal or abnormal regulation and integration of physiological mechanisms at all levels of biological organization, ranging from molecules to humans, including clinical investigations. It is published 12 times a year (monthly) by the American Physiological Society, 9650 Rockville Pike, Bethesda MD 20814-3991. Copyright © 2005 by the American Physiological Society. ISSN: 0363-6119, ESSN: 1522-1490. Visit our website at <http://www.the-aps.org/>.

Central nervous system origins of the sympathetic nervous system outflow to white adipose tissue

MARYAM BAMSHAD, VICTOR T. AOKI, M. GREGORY ADKISON,
WADE S. WARREN, AND TIMOTHY J. BARTNESS

Departments of Psychology and of Biology, Neuropsychology and Behavioral Neurosciences, and Neurobiology Programs, Georgia State University, Atlanta, Georgia 30303

Bamshad, Maryam, Victor T. Aoki, M. Gregory Adkison, Wade S. Warren, and Timothy J. Bartness. Central nervous system origins of the sympathetic nervous system outflow to white adipose tissue. *Am. J. Physiol.* 275 (*Regulatory Integrative Comp. Physiol.* 44): R291–R299, 1998.— White adipose tissue (WAT) is innervated by postganglionic sympathetic nervous system (SNS) neurons, suggesting that lipid mobilization could be regulated by the SNS [T. G. Youngstrom and T. J. Bartness. *Am. J. Physiol.* 268 (*Regulatory Integrative Comp. Physiol.* 37): R744–R751, 1995]. A viral transsynaptic retrograde tract tracer, the pseudorabies virus (PRV), was used to identify the origins of the SNS outflow from the brain to WAT neuroanatomically. PRV was injected into epididymal or inguinal WAT (EWAT and IWAT, respectively) of Siberian hamsters and IWAT of rats. PRV-infected neurons were visualized by immunocytochemistry and found in the spinal cord, brain stem (medulla, nucleus of the solitary tract, caudal raphe nucleus, C1 and A5 regions), midbrain (central gray), and several areas within the forebrain. The general pattern of infection of WAT in both species was more similar than different and resembled that seen after PRV injections into the adrenal medulla in rats (A. M. Strack, W. B. Sawyer, J. H. Hughes, K. B. Platt, and A. D. Loewy. *Brain Res.* 491: 156–162, 1989). EWAT versus IWAT injected hamsters had relatively less labeling in the suprachiasmatic, dorsomedial, and arcuate nuclei. Overall, it appeared that the SNS innervation of WAT originates from the general SNS outflow of the central nervous system and therefore may play a significant role in lipid mobilization.

pseudorabies virus; hamsters; rats; lipolysis; obesity; paraventricular nucleus; suprachiasmatic nucleus

LIPID IS MOBILIZED from adipocytes through the process of lipolysis under conditions where energy needs cannot be met by circulating fuels or stored carbohydrate. Lipolysis occurs in white adipose tissue (WAT) adipocytes when lipolytic neurotransmitters or hormones bind to their receptors, ultimately activating hormone-sensitive lipase that breaks triglycerides down to glycerol and fatty acids (24). Traditionally, investigations of the stimuli that initiate the lipolytic cascade have focused on the role of humoral substances, such as adrenal medullary-released catecholamines (28, 44), or a variety of hormones, including glucagon (e.g., Ref. 19).

Physiological evidence strongly suggests that the sympathetic nervous system (SNS) also is involved in the regulation of lipolysis and the mobilization of lipid stores from WAT. For example, cold exposure in laboratory rats increases norepinephrine (NE) turnover in WAT and increases circulating free fatty acid concentrations, responses that are not blocked by adrenal demedullation (11). In fasted rats, NE turnover is increased in

WAT, but decreased in BAT (23). Recently, electrophysiological recordings of the sympathetic nerves that innervate WAT show decreases and increases in their firing rates in response to intravenous glucose infusions and 2-deoxy-D-glucose, respectively (25). Despite these and other findings, the significance of the role of the SNS innervation of WAT has been debated for over 100 years. This debate largely has continued because, until recently (see below; 45), there was no clear neuroanatomical evidence showing that WAT is directly innervated by the SNS.

We began our tests for the possible SNS innervation of WAT by studying Siberian hamsters (*Phodopus sungorus sungorus*). These animals were chosen because they show naturally occurring decreases in body fat when transferred from long, “summerlike” days (LDs) to short, “winterlike” days (SDs). Specifically, the more internally located fat pads [i.e., epididymal WAT (EWAT) and retroperitoneal WAT (RWAT)] show relatively greater decreases in fat pad mass than the more externally located subcutaneous fat [i.e., inguinal WAT (IWAT) and dorsosubcutaneous WAT; Ref. 1]. This differential pattern of lipid mobilization suggests distinct SNS innervation, as well as separate SNS drives on these pads. Indeed, when fluorescent retrograde tract tracers are injected into EWAT and IWAT pads, postganglionic SNS neurons are labeled in the sympathetic chain (45) and there is a nonoverlapping postganglionic distribution of neurons innervating these WAT pads. In addition, when fluorescent anterograde tract tracers are injected into the sympathetic chain ganglia, rings of fluorescence surround each adipocyte in the WAT pads (45). This relatively separate innervation of WAT depots appears to permit differential SNS drives on the tissue and therefore separate degrees of lipolysis, because NE turnover rates are correlated with the magnitude of the SD-induced fat pad mass decreases (45). It was not determined in this study, however, where the central nervous system (CNS) origins of the SNS outflow to the WAT pads were located, because of the multisynaptic nature of the SNS innervation of target tissues (21).

Therefore, the purpose of the present experiments was to determine the SNS outflow from the CNS to WAT. To define this circuitry, a viral transsynaptic retrograde tract tracer, the pseudorabies virus (PRV), was injected into WAT pads and the resulting viral infections were traced in the CNS. PRV is taken up into neurons after binding to viral attachment protein molecules found on the surface of neuronal membranes. The virus replicates within the infected cell, thereby acting as a self-amplifying cell marker (17, 36). It is

then transferred to neurons synapsing on the infected cell by a specific transneuronal mechanism, rather than by lateral spread to adjacent, but unrelated, neurons or by a nonsynaptic mechanism. This process continues, causing infections along the neuronal chain from the periphery to higher CNS sites (17, 36). These PRV-labeled neurons can be visualized using standard immunocytochemical techniques.

In the present study, we examined the CNS origins of the SNS innervation to WAT in Siberian hamsters. This species was chosen because WAT is clearly innervated by the SNS in these animals (45). We also conducted similar experiments in laboratory rats for two reasons: first, to test the species generality of the pattern of the defined connections; and second, because the majority of the previous neuroanatomical and physiological studies of the SNS innervation of WAT have been done using rats.

MATERIALS AND METHODS

Animals. Fifty-eight Siberian hamsters (*Phodopus sungorus sungorus*) and 20 rats were used in this study. Hamsters and rats were given Purina Rodent Chow (#5001, 3.4 kcal/g) and tap water ad libitum. Adult male Siberian hamsters were obtained from our breeding colony. Our original stock of hamsters, supplied by Dr. Bruce Goldman (University of Connecticut), was interbred in 1990 with wild-trapped hamsters supplied by Dr. Katherine Wynne-Edwards (Queen's University) and with hamsters from an isolated colony in 1995 (Dr. G. Robert Lynch, University of Colorado). The adult hamsters in our colony are group housed (10–12/cage) in polyvinyl cages (48 × 27 × 15 cm) and kept in an LD cycle that simulates long day, summerlike, conditions (16:8 LD with lights on at 0300). Food and water were available ad libitum. Adult male Sprague-Dawley rats were purchased from Charles River. They were group housed in cages (5/cage; 48 × 27 × 20 cm) and were kept, in a separate room, under the same conditions as the Siberian hamsters.

Surgical procedures. Animals were anesthetized with pentobarbital sodium (50 mg/kg). The IWAT or the EWAT was exposed. The attenuated strain of the Bartha gC^{Ka} PRV (initially supplied by Dr. Arthur Loewy; Washington University, St. Louis, and then by Dr. Teryl Frey, Georgia State University) was injected into right IWAT or EWAT pads. In hamsters, the PRV [1.0×10^8 plaque forming units (pfu) per milliliter] was injected in 120-nl volumes into five areas across the length of the IWAT pad ($n = 50$) or EWAT pad ($n = 8$). In rats, because IWAT pads are larger compared with hamsters, the PRV was injected at a higher concentration (3.0×10^8 pfu/ml) and in higher volumes (300 nl) into eight areas across the length of the fat pad ($n = 20$). All surgical procedures were done under a fume hood in the morning between 0900 and 1100. After the surgery, animals were placed singly in cages (23 × 26 × 20 cm) with microisolator filter tops, and each species was housed in a room separate from noninjected animals. The time course for PRV infection rate was determined by killing the animals at various intervals after PRV injections. All animals were killed in the morning between 0900 and 1100. Hamsters with injections into IWAT were perfused intracardially with 4% paraformaldehyde at intervals of 3 ($n = 4$), 4 ($n = 30$), 5 ($n = 8$), or 6 ($n = 8$) days after surgery. Because the most extensive infections were seen in animals killed 6 days after injection, the rest of the hamsters with injections into the EWAT ($n = 8$) were perfused after 6 days. The time course for PRV infection rate

in rats injected into the IWAT also was determined by perfusing them at intervals of 6 ($n = 6$), 8 ($n = 8$), and 12 ($n = 6$) days after surgery.

Immunocytochemical procedures. The spinal cord and brain of each animal were postfixed overnight in 4% paraformaldehyde. The tissues were then placed in 25% sucrose overnight, cut in 50- μ m sections on a freezing microtome, and placed in 0.1 M sodium phosphate buffer with 0.1% sodium azide. A quintet of consecutive sections was processed for immunocytochemical visualization of PRV. Briefly, the sections were incubated in a pig polyclonal antibody to PRV (donated by Dr. Kenneth Platt, Iowa State University) overnight at room temperature. The PRV antibody was diluted 1:30,000 in a buffer solution containing 2% normal rabbit serum and 0.3% Triton X-100. The sections were then incubated in biotinylated rabbit anti-pig antibody (Sigma), at a 1:100 dilution for 2 h at room temperature. Next, the sections were incubated in the avidin-biotin horseradish peroxidase (HRP) complex (Vectastain ABC Elite Kit, Vector Laboratories, Burlingame, CA) at a 1:200 dilution for 1 h at room temperature. The HRP was visualized with 3–3-diaminobenzidine (DAB) and 6% H₂O₂ for 5 min. The sections were cleared with xylene and were placed under a coverslip with DPX.

The specificity of the immunocytochemical staining for the pig anti-PRV antibody used in this study has been previously validated (38).

Histological quantification. The PRV-labeled neurons were localized and quantified in IWAT and EWAT of Siberian hamsters using Image Tracer software (Translational Technology) and a stage-mounted position transducer system (MD3 Microscope Digitizer, Minnesota Datametrics). Camera lucida pictures of each brain section, stained with cresyl violet, were drawn and scanned into the computer. A digital image of each drawing was projected onto the computer screen using the Image Tracer program. The image of each brain section was registered with the same section on the microscope stage using the stage transducers. For all animals, the position of PRV-labeled neurons on each brain section was visualized with the microscope and was marked in the exact position on the computerized image of that section. The number of marked PRV-labeled neurons was counted in each nucleus for each animal.

RESULTS

There was no sign of sickness in any animals after PRV injection. Of 58 hamsters injected with PRV, 21 became infected. Examination of the brain tissue of the IWAT-injected animals showed that the spread of infection in the brain stem and midbrain increased with the length of the postinjection interval. Table 1 shows the average number of infected neurons in each brain region at various postinjection intervals. Hamsters injected with PRV into the IWAT and killed after 3 days showed no infection in the brain stem. After 4 days, neurons of the brain stem and midbrain were infected with the virus. After 5 or 6 days, neurons in the forebrain and hypothalamus also were infected. The highest number of neurons infected with the PRV was seen in the brain stem 6 days after injection. A similar pattern was seen for EWAT. Six days after PRV injection, the infection had spread to regions in the brain stem, midbrain, hypothalamus, and forebrain. The total number of neurons labeled with PRV was greater for IWAT than for EWAT in the majority of regions.

Table 1. Average number of transneuronally labeled neurons after injection of PRV into the EWAT and IWAT of the Siberian hamsters and the IWAT of rats

	Hamsters			Rats	
	IWAT			EWAT	IWAT
	4 days (n=13)	5 days (n=2)	6 days (n=3)	6 days (n=3)	8 days (n=4)
<i>Brain stem</i>					
Sol	0.0	22.5 ± 20.5	70.3 ± 35.3	63.0 ± 28.1	42.0 ± 16.0
Rob	0.8 ± 0.3	11.5 ± 2.5	27.3 ± 15.9	22.7 ± 14.8	26.2 ± 11.0
LRt	0.4 ± 0.2	10.0 ± 2.0	18.3 ± 10.7	3.7 ± 3.7	30.5 ± 12.0
C1/A1	0.0	2.5 ± 2.5	8.7 ± 4.9	2.7 ± 2.7	9.0 ± 2.7
RVL	4.9 ± 1.8	21.0 ± 7.0	43.3 ± 7.4	34.7 ± 18.3	35.5 ± 17.1
C1	3.2 ± 1.1	16.0 ± 3.0	53.7 ± 37.0	77.0 ± 47.5	48.0 ± 6.7
GiV	2.4 ± 1.4	14.0 ± 6.0	41.7 ± 26.0	8.0 ± 7.0	34.5 ± 5.0
GiA	3.2 ± 1.1	7.0 ± 2.0	68.6 ± 40.0	14.3 ± 7.3	50.2 ± 10.9
A5	3.2 ± 1.0	37.5 ± 24.5	28.3 ± 28.3	22.0 ± 10.4	25.8 ± 6.8
<i>Midbrain</i>					
CG	0.0	9.0 ± 9.0	10.3 ± 10.3	5.0 ± 3.2	14.5 ± 4.7
<i>Hypothalamus</i>					
DM	0.0	7.5 ± 7.5	4.3 ± 4.3	1.7 ± 1.7	8.8 ± 3.7
Arc	0.0	12.0 ± 12.0	1.7 ± 1.67	0.3 ± 0.3	5.8 ± 2.0
VMH	0.0	1.5 ± 1.5	2.7 ± 2.7	0.7 ± 0.7	3.5 ± 1.8
PVN	1.6 ± 1.0	37.0 ± 33.0	29.7 ± 27.7	33.3 ± 13.5	42.0 ± 7.1
SCN	0.0	4.0 ± 4.0	8.3 ± 8.3	1.0 ± 1.0	12.2 ± 3.8
MPA	0.0	36.5 ± 36.5	16.7 ± 16.7	43.0 ± 30.4	39.5 ± 6.6
Mfb	0.0	6.5 ± 6.5	3.3 ± 3.3	4.0 ± 4.0	5.2 ± 3.1
LS	0.0	0.0	1.0 ± 1.0	1.0 ± 1.0	9.5 ± 2.1

Values are means ± SE. PRV, pseudorabies virus; EWAT, IWAT, epididymal and inguinal, respectively, white adipose tissue; Sol, nucleus of the solitary tract; Rob, raphe obscurus nucleus; LRt, lateral reticular nucleus; RVL, rostroventrolateral reticular nucleus; C1, adrenaline cell; GiV, gigantocellular reticular nucleus, ventral part; GiA, gigantocellular reticular nucleus, alpha part; A5, noradrenaline cell; DM, dorsomedial hypothalamic nucleus; Arc, arcuate hypothalamic nucleus; VMH, ventromedial hypothalamic nucleus; PVN, paraventricular nucleus; SCN, supra-chiasmatic nucleus; MPA, medial preoptic area; CG, central gray; LS, lateral septum; Mfb, medial forebrain bundle; C1/A1, C1 adrenaline cell/A1 noradrenaline cell.

Spinal cord. Figure 1 shows a cross section of spinal cord in a Siberian hamster injected with PRV into the IWAT. The virus-labeled sympathetic preganglionic cells were localized in the intermediolateral (IML) cell group and the central autonomic nucleus. These virus-labeled cells were seen in a cluster ipsilateral to the injection site. The processes of the central autonomic nucleus neurons extended toward the IML cell group. PRV-

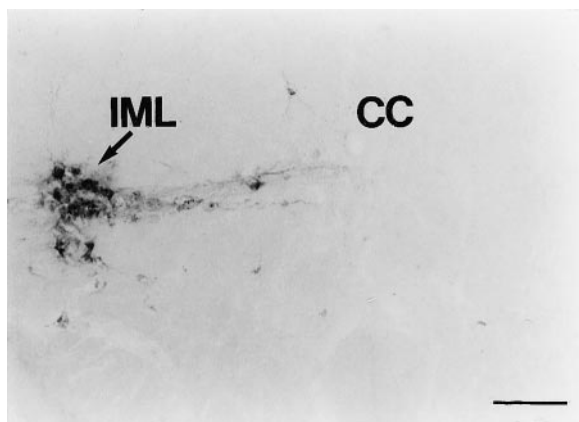


Fig. 1. Photomicrograph illustrating the distribution of pseudorabies virus (PRV)-labeled cells in cross section of spinal cord from a representative Siberian hamster 6 days after PRV injection into the inguinal white adipose tissue (IWAT). CC, central canal; IML, intermediolateral cell column. Bar 100 μ m.

immunoreactive particles were not seen in the extracellular areas, thus indicating that viral-induced lysis of infected neurons had not occurred.

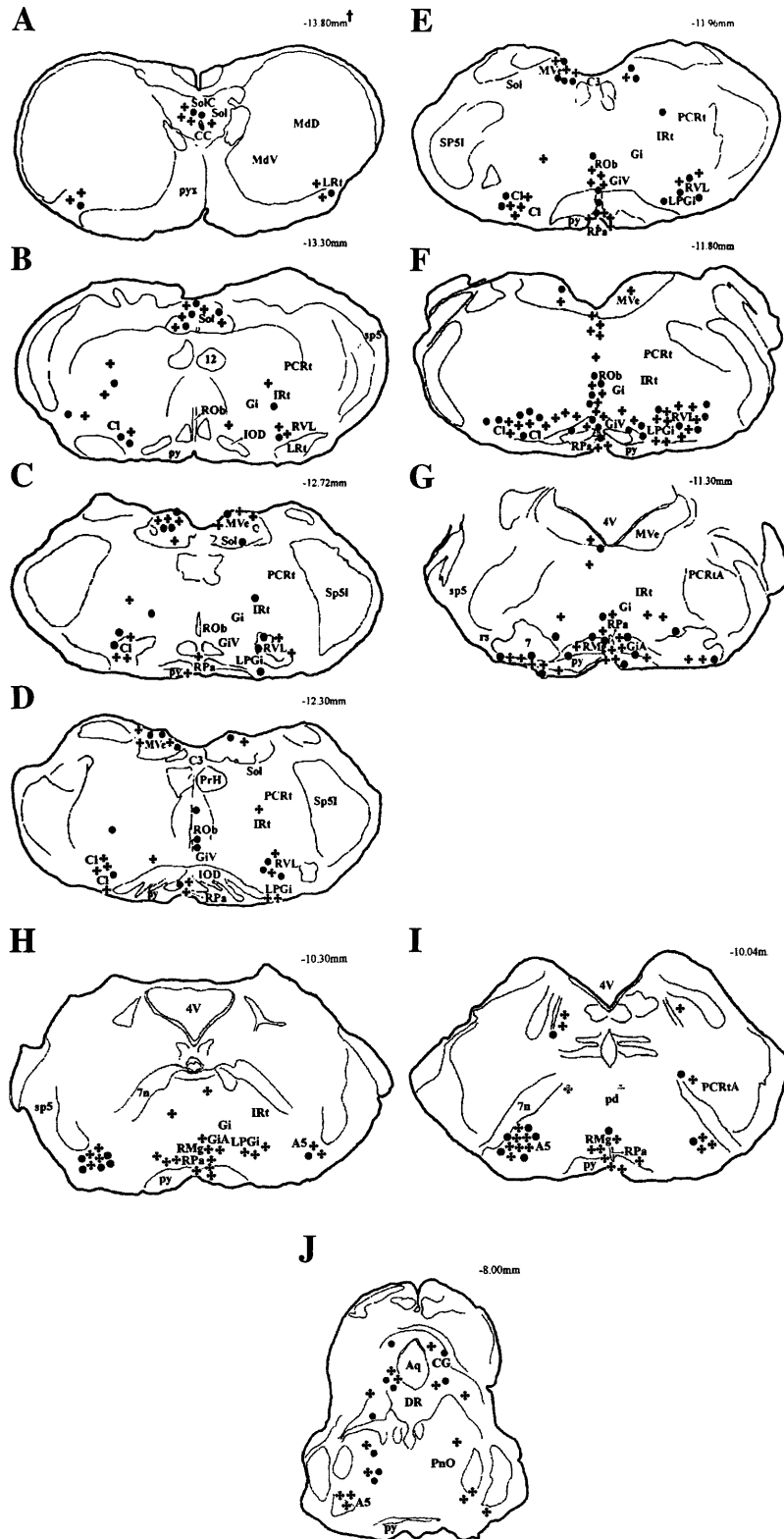
Figure 2, A–R, is a series of line drawings showing the rostrocaudal distribution of PRV-labeled cells from hamsters 6 days after injection of PRV into IWAT and EWAT. The pattern of PRV labeling in the brains of hamsters injected with the virus into IWAT or EWAT was quite similar. For both groups, the PRV labeling was bilateral, with more infected neurons seen ipsilateral to the injection site at levels above the spinal cord.

Brain stem. In the more caudal sections of the brain stem (Fig. 2, A–G), PRV-labeled cells for both IWAT and EWAT animals were seen mostly in the nucleus of the solitary tract, lateral and rostroventrolateral reticular nuclei, and the C1 region (at –13.80 to –13.30 mm levels). The dorsal portion of the medial vestibular nucleus also was infected with PRV neurons. Some PRV-infected neurons were seen in the caudal raphe, including raphe obscurus and raphe pallidus nuclei (at –12.72 to –11.30 mm levels). A few scattered neurons were found in the intermediate reticular nucleus. The majority of infected neurons were localized in the more rostral sections of the brain stem at the level of the prepositus hypoglossal nucleus (at –12.30 to –11.30 mm levels). At this level, PRV-infected neurons occupied the C1 region, the A5 region, rostroventrolateral reticular nucleus, and areas in the caudal raphe. The

ventral and alpha portions of the gigantocellular reticular nucleus and raphe magnus nucleus also had a large number of infected neurons.

At 6 days postinjection, there were some differences in the relative amount of infected neurons in some of the brain stem structures between the two PRV-injected WAT

pads in hamsters. The percentage of total labeled neurons was higher for EWAT versus IWAT in the nucleus of the solitary tract (38 vs. 16%) and lower in the lateral reticular nucleus (0.7 vs. 4%) and gigantocellular reticular nucleus (2 vs. 10%). For EWAT, the infected cells were concentrated primarily in two specific regions, the nucleus of the solitary



tract and C1 adrenaline cell group (38 and 26% of the total labeled neurons, respectively). For IWAT, the infected cells were distributed more evenly across the brain stem nuclei.

Midbrain. The PRV-infected neurons within the mid-brain were predominantly at the level of the facial nerve (at -10.30 to -10.04 mm levels; Fig. 2, *H-J*).

More rostrally, the dorsal and ventral portions of the central gray had PRV-labeled neurons.

Forebrain. PRV-infected neurons occupied several hypothalamic regions, specifically, the arcuate nucleus, ventral premammillary nucleus, dorsomedial nucleus of the hypothalamus (DMN), and dorsal hypothalamic

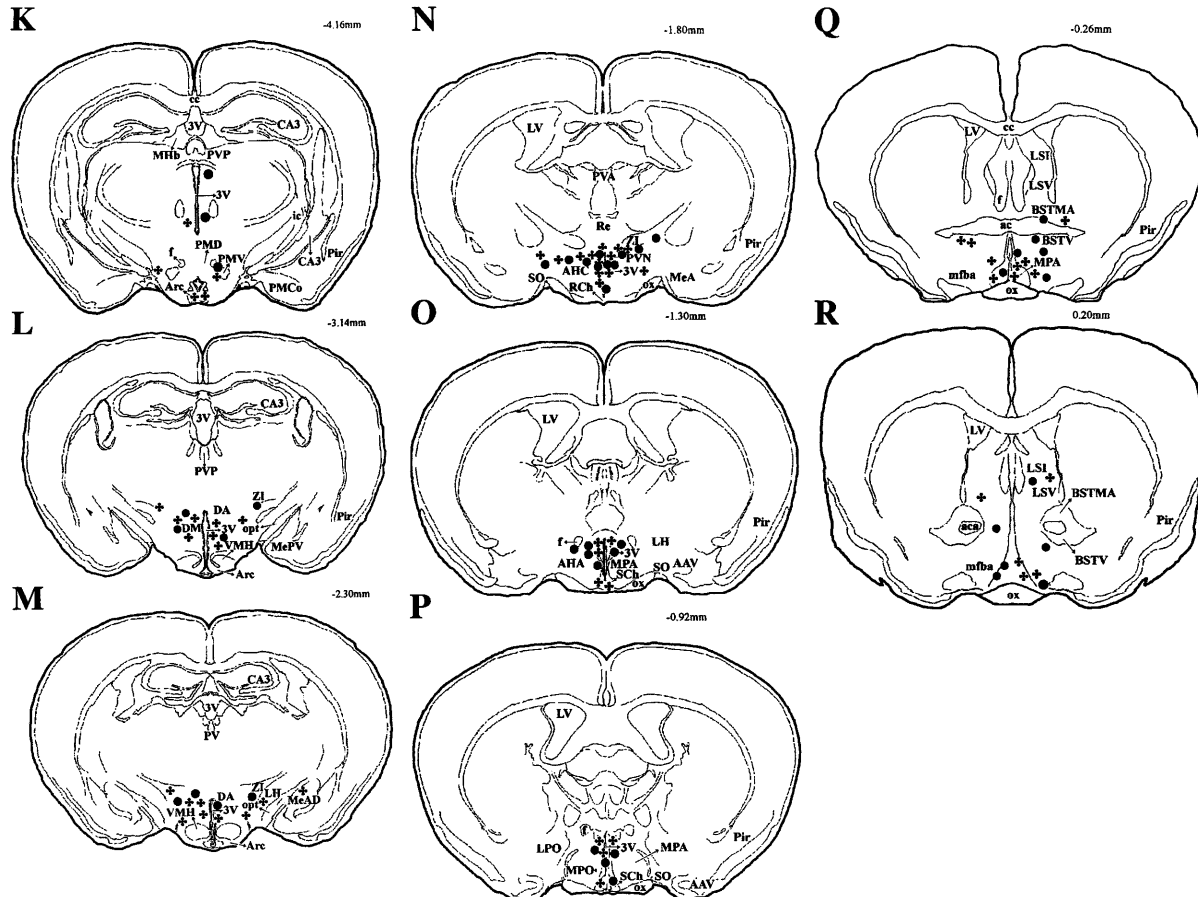


Fig. 2. Schematic diagrams showing the distribution of PRV-labeled cells in cross sections through the brain from caudal to rostral levels in Siberian hamsters 6 days after PRV injection into the right IWAT (+) or into the right epididymal white adipose tissue (EWAT; ●). Each symbol represents 1–8 infected neurons. † Bregma measurements copied from the rat atlas (27). 12, Hypoglossal nucleus; 3V, 3rd ventricle; 4V, 4th ventricle; 7, facial nucleus; 7n, facial nerve; A5, A5 noradrenaline cells; AAV, anterior amygdaloid area, ventral part; aca, anterior commissure, anterior part; AHA, anterior hypothalamic area, anterior part; AHC, anterior hypothalamic area, central part; Aq, aqueduct; Arc, arcuate hypothalamic nucleus; BSTMA, bed nucleus of the stria terminalis, medial division, anterior part; BSTV, bed nucleus of the stria terminalis, ventral division; C1, C1 adrenaline cells; C3, C3 adrenaline cells; CA3, CA3 of Ammon's horn; CC, central canal; cc, corpus callosum; cg, central gray; DA, dorsal hypothalamic area; DM, dorsomedial hypothalamic nucleus; DR, dorsal raphe nucleus; f, fornix; Gi, gigantocellular reticular nucleus; GiA, gigantocellular reticular nucleus, alpha part; GiV, gigantocellular reticular nucleus, ventral part; ic, internal capsule; IOD, inferior olive, dorsal nucleus; IRt, intermediate reticular nucleus; LH, lateral hypothalamic area; LPGi, lateral paragigantocellular nucleus; LPO, lateral preoptic area; LRt, lateral reticular nucleus; LSI, lateral septal nucleus, intermediate part; LSV, lateral septal nucleus, ventral part; LV, lateral ventricle; MdD, medullary reticular nucleus, dorsal part; MdV, medullary reticular nucleus, ventral part; MeA, medial amygdaloid nucleus, anterior part; MeAD, medial amygdaloid nucleus, anterodorsal part; MePV, medial amygdaloid nucleus, posterodorsal part; mfb, medial forebrain bundle; MHb, medial habenular nucleus; MPA, medial preoptic area; MPO, medial preoptic nucleus; MVe, medial vestibular nucleus; opt, optic tract; ox, optic chiasm; PCRt, parvocellular reticular nucleus; PCRtA, parvocellular reticular nucleus, alpha part; pd, predorsal bundle; Pir, piriform cortex; PMCo, posteromedial cortical amygdaloid nucleus; PMD, premammillary nucleus, dorsal part; PMV, premammillary nucleus, ventral part; PnO, pontine reticular nucleus, oral part; PrH, prepositus hypoglossal nucleus; PVA, paraventricular thalamic nucleus, anterior part; PVN, paraventricular hypothalamic nucleus; PVP, paraventricular thalamic nucleus, posterior part; py, pyramidal tract; pyx, pyramidal decussation; RCh, retrochiasmatic area; Re, reuniens thalamic nucleus; RMg, raphe magnus nucleus; ROb, raphe obscurus nucleus; RPa, raphe pallidus nucleus; rs, rubrospinal tract; RVL, rostroventrolateral reticular nucleus; RCh, supraoptic nucleus; SO, supraoptic nucleus; Sol, nucleus of the solitary tract; SolC, nucleus of the solitary tract, commissural part; sp5, spinal trigeminal tract; Sp5I, spinal trigeminal nucleus, interpolar part; VMH, ventromedial hypothalamic nucleus; ZI, zona incerta.

area (Fig. 2, *K-M*). Scattered cells were seen in the lateral hypothalamus, zona incerta, and medial amygdala. A few PRV-labeled cells were seen in the ventromedial hypothalamic nucleus (VMH). The percentage of total labeled cells was less in the DMN after PRV was injected into EWAT (1%) compared with IWAT (7%).

In the most rostral sections of the hypothalamus (Fig. 2, *N-R*), the majority of PRV-labeled cells was found in the medial and anterior parvocellular portion of the paraventricular nucleus and the medial preoptic nucleus. Some labeling, however, also occurred in the lateral magnocellular portion of the paraventricular nucleus (at -1.80 to -1.30 mm levels). PRV also infected neurons of the suprachiasmatic nuclei (SCN), but more so when the virus was injected into the IWAT than the EWAT, a finding reflected in the percentage of total labeled cells (4.2 vs. 0.6%, respectively). Overall, the correlation for the absolute numbers of infected neurons across hypothalamic sites was significant between hamsters injected with virus in IWAT and EWAT ($r = 0.74$; $P < 0.05$).

In the nonhypothalamic forebrain, PRV labeling was seen in the zona incerta and medial amygdala, but was most dense in the medial preoptic area (MPOA), with some cells scattered in the medial forebrain bundle, ventral septum, and medial and ventral divisions of the bed nucleus of the stria terminalis (at -0.26 to 0.20 mm levels).

Species comparison. In comparison to Siberian hamsters, a higher dilution and volume of PRV had to be injected into the IWAT to infect the laboratory rats. The most extensive infection was seen in rats killed 12 days after PRV injection. Despite these differences in virility of PRV between rats and hamsters, the pattern of PRV labeling after IWAT injection was quite similar between these two rodent species. Figure 3, *A-C* and *D-F*, are photomicrographs of the rostrocaudal distribution of PRV-infected neurons in the brain of a representative Siberian hamster and a rat, respectively. No striking differences were seen between hamsters and rats in regions infected by PRV in the brain stem (Fig. 3, *A* and *D*), midbrain (Fig. 3, *B* and *E*), or hypothalamus (Fig. 3, *C* and *F*).

DISCUSSION

Injections of PRV into WAT pads of Siberian hamsters and laboratory rats labeled a chain of functionally connected neurons extending from the forebrain to the WAT pads, including several hypothalamic, midbrain, and brain stem regions, as well as the spinal cord. These data represent the first neuroanatomical evidence of CNS connections to WAT. A large body of literature has implied that the CNS is functionally connected to WAT. This notion was based on the effects of electrical stimulation or lesions of brain sites on WAT mass (see below). The results of the present study show PRV labeling of neurons in areas of the spinal cord, brain stem, midbrain, and forebrain and support some, but not all, of the neuroanatomically and functionally implicated origins of the SNS outflow to the periphery. The pattern of infected neurons in hamsters and rats after PRV injections into WAT was strikingly similar to

that found after PRV injections into the adrenal medulla or sympathetic ganglia of rats. (We have injected PRV into the adrenal gland of hamsters and found the same pattern of infection as in rats; unpublished data.) That is, PRV injections into the adrenal medulla infect neurons in several medullary regions such as the rostral ventrolateral and rostral ventromedial medulla and the A5 and the caudal raphe region of the brain stem (17, 37, 38). These data, as well as our previous finding that postganglionic neurons of the sympathetic chain innervate WAT (45), strongly support the view that the CNS sites labeled in the present experiment are part of the SNS innervation of WAT.

It is not surprising that PRV injections into WAT infected neurons in the dorsal and medial subdivisions of the PVN, because these subdivisions project to the spinal preganglionic neurons (16, 22, 31, 32). In addition, the PVN is implicated in the control of lipid mobilization (e.g., Ref. 4). Some of the other forebrain areas labeled after PRV injections into WAT were the SCN, MPOA, and DMN. These areas also have been implicated in the control of lipid mobilization (see below).

The SCN is the primary biological clock in many mammals that, among its many functions, regulates the 24-h rhythm of metabolism (15). The role of SCN in lipid mobilization has been shown in studies involving microknife cuts. Microknife cuts that deafferent the forebrain just behind the SCN block 2-deoxy-D-glucose-, fasting-, forced exercise-, and cold exposure-induced increases in lipid mobilization (39). In addition, cycles of lipogenesis and lipolysis in rats and mice, as reflected by their respiratory quotient, have a 24-h rhythm, suggesting that the SCN is involved in regulation of these processes (9, 20). Moreover, the SCN is further implicated as affecting SCN outflow to the peripheral tissues, such as WAT, because SCN lesions disrupt the circadian rhythm of NE turnover (i.e., SNS drive) in the adrenal and pineal glands, liver, heart, and kidney (43). The labeled neurons in the SCN after PRV injections into WAT reinforce the hypothesis that the SCN neurons are part of the SNS outflow from the brain to WAT. Therefore, it may be that the connections between the SCN and WAT control the daily peaks and nadirs of lipid mobilization through variations in the sympathetic drive on this tissue.

The DMN of the hypothalamus, like the PVN (for review, see Ref. 34), has been implicated in the control of food intake, body mass, linear growth (for review, see Ref. 3), and, most importantly for the present discussion, mobilization of peripheral lipid stores (46). Specifically, injections of NE into the DMN of rats elicit increases in plasma free fatty acid concentrations (46). This apparent increase in lipid mobilization may occur because the DMN neurons are connected to WAT via the SNS preganglionic neurons. The results of the present study provide a neuroanatomical basis for such a connection. Indeed, the SNS preganglionic neurons could be innervated by the DMN through several routes, including a direct dopaminergic projection to the spinal cord (6) and other projections to the thoracic spinal cord (31, 32), as well as an indirect connection to

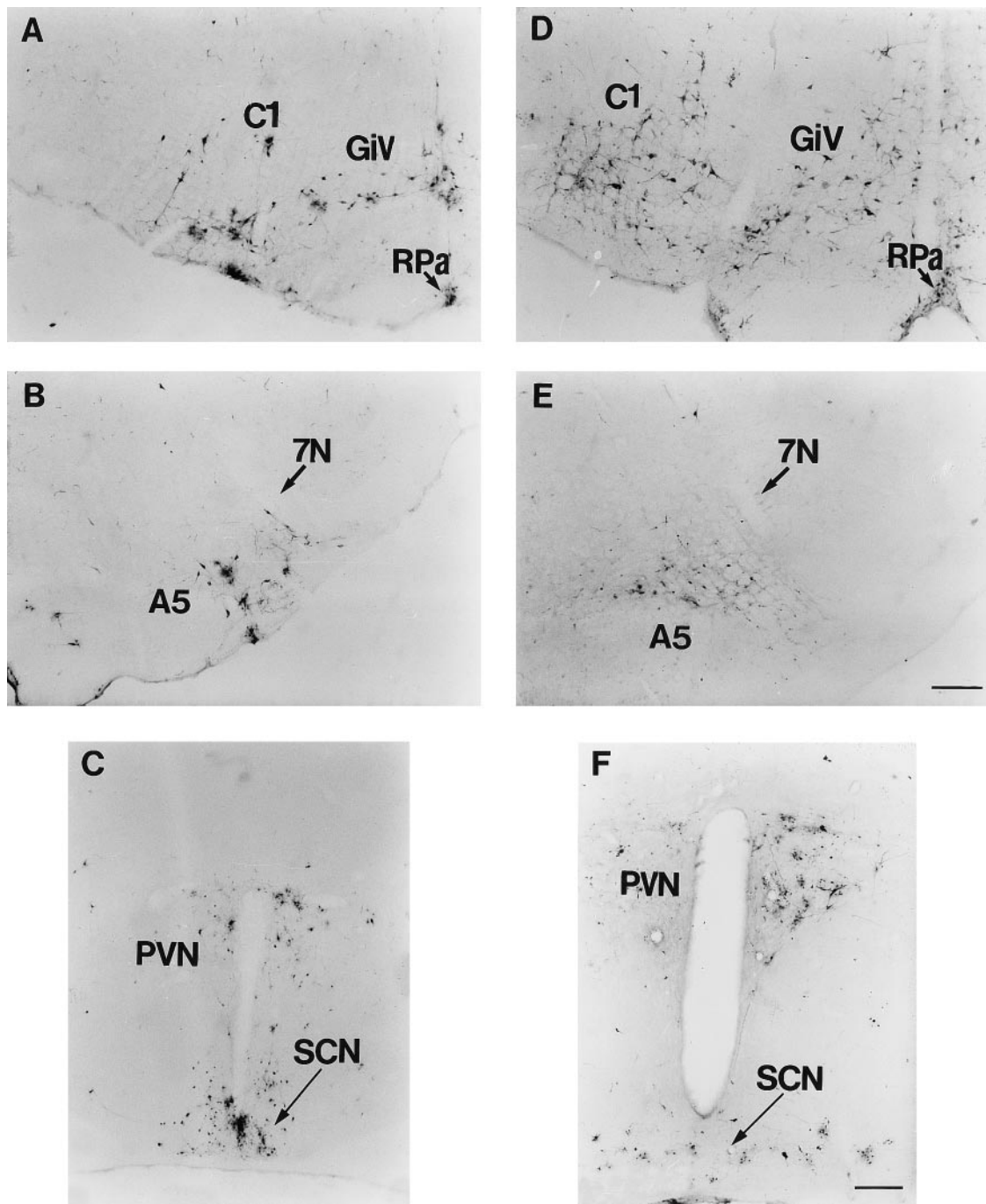


Fig. 3. Photomicrographs illustrating the distribution of PRV-labeled cells in cross sections of brain from a representative Siberian hamster and a representative rat 6 days after PRV injection into the IWAT. *A* and *D*: brain stem of a Siberian hamster and a laboratory rat, respectively. *B* and *E*: midbrain of a Siberian hamster and a rat, respectively. Bar 200 μ m. *C* and *F*: hypothalamus of a Siberian hamster and a rat, respectively. SCN, suprachiasmatic nucleus. Bar 200 μ m.

the parvocellular paraventricular nucleus and then to the spinal cord (40).

Lesions of the MPOA impair the mobilization of free fatty acids after cold exposure (7). This effect has been attributed to a role of this area in the SNS outflow to WAT or the adrenal medulla. Labeling of MPOA neurons after PRV injection into WAT, shown in the present study, provides direct neuroanatomical evidence for existence of this hypothesized connection. The exact connections of the

MPOA to the sympathetic spinal preganglionics are not known.

The VMH have been implicated repeatedly in the control of WAT lipid mobilization based on the effects of brain lesions or electrical or chemical stimulation of this structure. For example, rats bearing lesions of the VMH have a decreased lipolytic rate in response to fasting, forced exercise (swimming), cold exposure, and injections of 2-deoxy-D-glucose (26). Moreover, VMH

lesions inhibit fasting-induced mobilization of lipid from ipsilateral RWAT in laboratory rats, an effect that can be mimicked by unilateral SNS denervation of this fat pad (26). Furthermore, VMH lesions decrease the SNS drive on WAT (41). It should be recalled, however, that we found very few infected neurons in the VMH and, in most animals, none at all. Thus we believe that, in an attempt to ensure complete destruction of the VMH, the large lesions that typically are made most likely produced ancillary damage to neural elements involved in the SNS outflow from the brain to WAT. Specifically, these neural elements might include the DMN and PVN of the hypothalamus (see above) or their efferents, because they are part of the SNS outflow from the CNS to peripheral targets generally (37, 38) and from the CNS to WAT specifically (present experiments). This misplaced focus on the VMH is reminiscent of the "myth of the VMH" (12) that resulted originally from the emphasis on these nuclei in relationship to the control of body fat and food intake (e.g., Ref. 8). We now know that the effects of VMH lesions on body and lipid mass and food intake are due primarily to the destruction of the descending projections from the PVN that course just lateral to the VMH (12, 13, 18, 33, 34). We recognize that there are differences in the so-called VMH and PVN syndromes with regard to food intake and body mass, however. The presumed effects of VMH lesions on WAT mobilization, as well as the effects of stimulation of the VMH on this response also may be due to involvement of the descending autonomic pathways from the PVN to WAT.

The current data do not address the exact circuitry involving the many areas of infected neurons in the CNS and their relationship to the spinal preganglionic SNS neurons that project to the sympathetic chain and then terminate in the WAT pads. Our previous work with the retrograde tract tracer FluoroGold (45) demonstrated relatively separate innervation of IWAT and EWAT at the level of the sympathetic chain. In the present study, we found some differences in the pattern of SNS connections to the IWAT and EWAT. It is unlikely that differences in amount of infection between IWAT and EWAT seen in some brain sites were due merely to differences in length of PRV transfer from the fat pads to the CNS. As seen in Table 1, rostral areas such as the MPOA had more infected neurons after PRV injections into the EWAT than IWAT, despite the fact that the virus would have had to travel farther to get to this region of the neuroaxis than after PRV injections into IWAT. Although there were some differences between IWAT versus EWAT injections of the virus, more similarities than differences in labeling were seen (Table 1). Therefore, it may be that convergence of the SNS outflow occurs from the forebrain to and through the brain stem, but the relatively separate postganglionic innervation of WAT (45) explains the differential rates of lipid mobilization among WAT pads (e.g., Refs. 14 and 42).

As discussed above, the foremost factor that prompted us to examine differences in the SNS innervation of WAT

pads in Siberian hamsters using the PRV method was 1) relatively discrete postganglionic neuronal innervation of the EWAT and IWAT pads (45) and 2) differential rates of SNS drive on these pads, as indicated by separate NE turnover rates (45). Some differences in the extent of labeling were seen after PRV injections into these pads (see Table 1); however, their significance relies on the functional role of the labeled structures in the mobilization of lipid by the two pads and may be possible to determine using stimulation and/or lesion techniques.

Perspectives

The present data do not address the type of connections between the brain and WAT. Specifically, although the first histological evidence that WAT is innervated was shown almost a 100 years ago (10), controversy exists as to whether the nerves innervate the fat cells or the vasculature. The most convincing evidence for the dual innervation of fat cells and the vasculature was gathered by combining the histofluorescence technique with confocal microscopy (29); unfortunately, these data only appear in a preliminary form within a review and without pictures or quantification. This study reported that, in rats, catecholaminergic neural fluorescence was seen in direct contact with fat cells (in EWAT, IWAT, perirenal WAT, and mesenteric WAT) in addition to the vasculature in these pads (29).

If fat cells are directly innervated, or are indirectly innervated via en passant nerve endings, then the mechanism by which NE release stimulates lipolysis is quite conventional and could be easily envisioned and understood. Rosell (30) has suggested, however, that the sympathetic neurons innervate the epithelial lining of the vasculature and, with SNS stimulation, increase vascular permeability. This poses an interesting alternative as to the means by which the SNS might promote lipolysis indirectly. SNS stimulation could increase the permeability of albumin, allowing it to accept free fatty acids liberated from adipocytes. This would have the effect of removing the inhibition of lipolysis that occurs with increases in extracellular free fatty acid concentrations (30). Thus a higher rate of lipolysis would be permitted and mediated through the SNS innervation of WAT on the vasculature. Regardless of the exact connections between the SNS and WAT components, it appears likely that the SNS innervation of WAT is important for the physiological control of lipolysis.

The authors especially thank Dr. Arthur Loewy for help and encouragement, as well as Drs. Patrick Card, Michael Stock, George Wade, Neil Rowland, and Terry Powley for helpful discussions of these data. Moreover, we thank Dr. Arthur S. P. Jansen for guidance in the use of PRV and Mary Margaret Mauer for comments on the manuscript. We also thank Dr. Kenneth Platt (Iowa State University) for the gift of the antibodies.

This work was supported in part by National Institute of Diabetes and Digestive and Kidney Diseases Grant RO1-DK-35254, National Institute of Mental Health Research Scientist Development Award KO2-MH-00841 to T. J. Bartness, and by the State of Georgia Chancellor's Initiative Fund.

Address for reprint requests: T. J. Bartness, Dept. of Psychology, Georgia State Univ., Atlanta, GA 30303.

Received 25 July 1997; accepted in final form 6 April 1998.

REFERENCES

1. **Bartness, T. J., J. M. Hamilton, G. N. Wade, and B. D. Goldman.** Regional differences in fat pad responses to short days in Siberian hamsters. *Am. J. Physiol.* 257 (*Regulatory Integrative Comp. Physiol.* 26): R1533–R1540, 1989.
3. **Bernardis, L. L., and L. L. Bellinger.** The dorsomedial hypothalamic nucleus revisited: 1986 update. *Brain Res. Rev.* 12: 321–381, 1987.
4. **Bray, G. A., A. Sclafani, and D. Novin.** Obesity-inducing hypothalamic knife-cuts: effects on lipolysis and blood insulin levels. *Am. J. Physiol.* 243 (*Regulatory Integrative Comp. Physiol.* 12): R455–R449, 1982.
5. **Cantu, R. C., and H. M. Goodman.** Effects of denervation and fasting on white adipose tissue. *Am. J. Physiol.* 212: 207–212, 1967.
6. **Cechetto, D. F., and C. B. Saper.** Neurochemical organization of the hypothalamic projection to the spinal cord in the rat. *J. Comp. Neurol.* 272: 579–604, 1988.
7. **Coimbra, C. C., and R. H. Migliorini.** Cold-induced free fatty acid mobilization is impaired in rats with lesions in preoptic area. *Neurosci. Lett.* 88: 1–5, 1988.
8. **Corbit, J. D., and E. Stellar.** Palatability, food intake and obesity in normal and hyperphagic rats. *J. Comp. Physiol. Psychol.* 58: 63–67, 1964.
9. **Cornich, S., and C. Cattene.** Fatty acid synthesis in mice during the 24 hr cycle and during meal feeding. *Horm. Metab. Res.* 10: 276–290, 1978.
10. **Dogiel, A. S.** Die sensiblen Nervenendigungen im Herzen und in den Blutgefassen der Säugethiere. *Arch. Mikrosk. Anat.* 52: 44–70, 1898.
11. **Garofalo, M. A. R., I. C. Kettelhut, J. E. S. Roselino, and R. H. Migliorini.** Effect of acute cold exposure on norepinephrine turnover rates in rat white adipose tissue. *J. Auton. Nerv. Syst.* 60: 206–208, 1996.
12. **Gold, R. M.** Hypothalamic obesity: the myth of the ventromedial nucleus. *Science* 182: 488–490, 1973.
13. **Gold, R. M., A. P. Jones, and P. E. Sawchenko.** Paraventricular area: critical focus of a longitudinal neurocircuitry mediating food intake. *Physiol. Behav.* 18: 1111–1119, 1977.
14. **Hartman, A. D., and D. W. Christ.** Effect of cell size, age and anatomical location on the lipolytic response of adipocytes. *Life Sci.* 22: 1087–1096, 1978.
15. **Hastings, M. H.** Circadian rhythms: peering into the molecular clockwork. *J. Neuroendocrinol.* 7: 331–340, 1995.
16. **Hosoya, Y., Y. Sugiura, N. Okada, A. D. Loewy, and K. Kohno.** Descending input from the hypothalamic paraventricular neurons to sympathetic preganglionic neurons in the rat. *Exp. Brain Res.* 85: 10–20, 1991.
17. **Jansen, A. S. P., D. G. Farwell, and A. D. Loewy.** Specificity of pseudorabies virus as a retrograde marker of sympathetic preganglionic neurons: implications for transneuronal labeling studies. *Brain Res.* 617: 103–112, 1993.
18. **Kirchgessner, A. L., and A. Sclafani.** PVN-hindbrain pathway involved in the hypothalamic hyperphagia-obesity syndrome. *Physiol. Behav.* 42: 517–528, 1988.
19. **Lefebvre, P., A. Luyckx, and Z. M. Bacq.** Effects of denervation on the metabolism and the response to glucagon of white adipose tissue of rats. *Horm. Metab. Res.* 5: 245–250, 1973.
20. **LeMagnen, J., and M. Devos.** Metabolic correlates of the meal onset in the free food intake of rats. *Physiol. Behav.* 5: 805–814, 1970.
21. **Loewy, A. D.** Anatomy of the autonomic nervous system: an overview. In: *Central Regulation of Autonomic Functions*, edited by A. D. Loewy and K. M. Spyer. New York: Oxford Univ. Press, 1990, p. 3–16.
22. **Luiten, P. G. M., G. J. ter Horst, H. Karst, and A. B. Steffens.** The course of paraventricular hypothalamic efferents to autonomic structures in medulla and spinal cord. *Brain Res.* 329: 374–378, 1985.
23. **Migliorini, R. H., M. A. R. Garofalo, and I. C. Kettelhut.** Increased sympathetic activity in rat white adipose tissue during prolonged fasting. *Am. J. Physiol.* 272 (*Regulatory Integrative Comp. Physiol.* 41): R656–R661, 1997.
24. **Newsholme, E. A., and A. R. Leech.** *Biochemistry for the Medical Sciences*. Chichester, UK: Wiley, 1983.
25. **Nijijima, A.** The effect of glucose and other sugars on the efferent activity of the sympathetic nerves innervating fatty tissue. *Jpn. J. Physiol.* 47, Suppl. 1: S40–S42, 1997.
26. **Nishizawa, Y., and G. A. Bray.** Ventromedial hypothalamic lesions and the mobilization of fatty acids. *J. Clin. Invest.* 61: 714–721, 1978.
27. **Paxinos, G., and C. Watson.** *The Rat Brain in Stereotaxic Coordinates*. Orlando, FL: Academic, 1986.
28. **Pecquery, R., M.-C. Leneuve, and Y. Giudicelli.** In vivo desensitization of the beta, but not the alpha-2-adrenoreceptor-coupled-adenylate cyclase system in hamster white adipocytes after administration of epinephrine. *Endocrinology* 114: 1576–1583, 1984.
29. **Rebuffe-Scrive, M.** Neuroregulation of adipose tissue: molecular and hormonal mechanisms. *Int. J. Obes.* 15: 83–86, 1991.
30. **Rosell, S.** Neuronal control of microvessels. *Annu. Rev. Physiol.* 42: 359–371, 1980.
31. **Saper, C. B., A. D. Loewy, L. W. Swanson, and W. M. Cowan.** Direct hypothalamo-autonomic connections. *Brain Res.* 117: 305–312, 1976.
32. **Sawchenko, P. E., and L. W. Swanson.** Immunohistochemical identification of neurons in the paraventricular nucleus of the hypothalamus that project to the medulla or to the spinal cord in the rat. *J. Comp. Neurol.* 205: 260–272, 1982.
33. **Sclafani, A.** Neural pathways involved in the ventromedial hypothalamic lesion syndrome in the rat. *J. Comp. Physiol. Psychol.* 77: 70–96, 1971.
34. **Sclafani, A., C. N. Berner, and G. Maul.** Feeding and drinking pathways between the medial and lateral hypothalamus in the rat. *J. Comp. Physiol. Psychol.* 85: 29–51, 1973.
35. **Steffens, A. B., J. H. Strubbe, B. Balkan, and A. J. W. Scheurink.** Neuroendocrine factors regulating blood glucose, plasma FFA and insulin in the development of obesity. *Brain Res. Bull.* 27: 505–510, 1991.
36. **Strack, A. M., and A. D. Loewy.** Pseudorabies virus: a highly specific transneuronal cell body marker in the sympathetic nervous system. *J. Neurosci.* 10: 2139–2147, 1990.
37. **Strack, A. M., W. B. Sawyer, J. H. Hughes, K. B. Platt, and A. D. Loewy.** A general pattern of CNS innervation of the sympathetic outflow demonstrated by transneuronal pseudorabies viral infections. *Brain Res.* 491: 156–162, 1989.
38. **Strack, A. M., W. B. Sawyer, K. B. Platt, and A. D. Loewy.** CNS cell groups regulating the sympathetic outflow to adrenal gland as revealed by transneuronal cell body labeling with pseudorabies virus. *Brain Res.* 491: 274–296, 1989.
39. **Teixeira, V. L., J. Antunes-Rodrigues, and R. H. Migliorini.** Evidence for centers in the central nervous system that selectively regulate fat mobilization in the rat. *J. Lipid Res.* 14: 672–677, 1973.
40. **Ter Horst, G. J., and P. G. M. Luiten.** The projections of the dorsomedial hypothalamic nucleus in the rat. *Brain Res. Bull.* 16: 231–248, 1986.
41. **Vander Tuig, J. G., J. Kerner, and D. R. Romsos.** Hypothalamic obesity, brown adipose tissue, and sympathoadrenal activity in rats. *Am. J. Physiol.* 248 (*Endocrinol. Metab.* 11): E607–E617, 1985.
42. **Wahrenberg, H., F. Lonnqvist, and P. Arner.** Mechanisms underlying regional differences in lipolysis in human adipose tissue. *J. Clin. Invest.* 84: 458–467, 1989.
43. **Warren, W. S., T. H. Champney, and V. M. Cassone.** The hypothalamic suprachiasmatic nucleus regulates circadian changes in norepinephrine turnover in sympathetically innervated tissue. *Soc. Neurosci. Abstr.* 21: 178, 1995.
44. **Wool, I. B., M. S. Goldstein, E. R. Ramey, and B. Levine.** Role of epinephrine in the physiology of fat mobilization. *Am. J. Physiol.* 178: 427–432, 1954.
45. **Youngstrom, T. G., and T. J. Bartness.** Catecholaminergic innervation of white adipose tissue in the Siberian hamster. *Am. J. Physiol.* 268 (*Regulatory Integrative Comp. Physiol.* 37): R744–R751, 1995.
46. **Zaia, C. T. B. V., L. C. J. Gaziri, D. A. M. Zaia, E. Delattre, M. S. Dolnikoff, and C. Timo-Iaria.** Effect of chemical stimulation of the dorsomedial hypothalamic nucleus on blood plasma glucose, triglycerides and free fatty acids in rats. *Brain Res. Bull.* 42: 195–198, 1997.